Measurement of the half-life of excited nuclear states using liquid scintillation counting

Chavdar Dutsov[a,*], Benoit Sabot[b], Philippe Cassette[a], Krasimir Mitev[a]

[a] *Sofia University "St. Kliment Ohridski", Faculty of Physics, 5 James Bourchier Blvd, 1164 Bulgaria*
[b] *Université Paris-Saclay, CEA, LIST, Laboratoire National Henri Becquerel (LNE-LNHB), F-91120 Palaiseau, France*

Abstract

This work presents measurements of the half-lives of excited nuclear states of ^{237}Np and ^{57}Fe using a liquid scintillation (LS) spectrometer and a gamma detector. A novel approach for the determination of the half-lives of some excited states is presented which uses only LS counting data from a detector with two PMTs. The lifetime of the 1st and 2nd excited states of ^{57}Fe were obtained without the use of a gamma detector. The obtained value for the 59.54 keV level of ^{237}Np is 67.60(25) ns. The obtained values for the 14.4 keV and 136.5 keV levels of ^{57}Fe are 97.90(40) ns and 8.780(36) ns, respectively. The half-life results from this study are consistent with the average value found in the reference decay data tables and have a lower uncertainty.

Keywords: Half-life measurements, LSC, Np-237, Fe-57, Liquid scintillation

1. Introduction

Liquid scintillation (LS) counting is a powerful method for measurement of activity of α, β emitting and electron capture (EC) radionuclides and is widely used in laboratories around the world. It is particularly suited to the detection of low-energy beta emitters due to its 4π geometry and high detection efficiency, which is practically 100% for electrons with energies over 40 keV (L'Annunziata, 2012). The measurements are usually performed with an aliquot of an aqueous solution, containing the radionuclide, which is dissolved in an organic scintillator and placed in a glass or a plastic vial. The scintillation light is then detected by two or more photomultiplier tubes (PMTs) working in coincidence.

LS counting is well suited for half-life measurements of radioisotopes. In the recent years it was successfully used in combination with mass spectrometry for the accurate determination of the half-lives of ^{147}Sm (1.08×10^{11} years) (Kossert et al., 2009), ^{176}Lu (3.8×10^{10} y) (Kossert et al., 2013), ^{10}Be (1.4×10^{6} y) (Chmeleff et al., 2010). It was also used for the direct measurement of the half-lives of ^{212}Pb (10.64 h) (Kossert, 2017), ^{213}Po (3.7 µs) (Kossert et al., 2020) and others. The range covers half-lives from several microseconds to 10^{11} years.

Due to the fast response of organic scintillators (typically a few ns, depending on the scintillator) and PMTs (typically 1.3 ns rise time), the timing of scintillation events could be very precise. These factors, in combination with the high detection efficiency and favorable geometry of LS counting, make it a useful method for fast timing measurements in the nanosecond range.

In this work we show that the LS method could be a useful tool to study the half-lives of nuclear isomeric states. Two measurement techniques are proposed: one which utilizes a 3-PMT LS counting detector equipped with additional γ detector and a CAEN digitizer and another with a 2-PMT LS counting detector – without the use of a γ channel. We analyze the time interval distributions between the events in the different channels of the system and demonstrate that these could be used for accurate determination of the half-lives of some excited states in certain nuclides.

2. Materials and methods

Two experimental systems were used in this study. An integral part of both systems is a CAEN DT5751 desktop digitizer, which is used to digitize all incoming signals and write their timestamp in list-mode files. The systems will be described in short hereafter.

2.1. 3-PMT & γ detection system

The first experimental system is a portable LS counter developed at French national metrology laboratory (LNE-LNHB) for primary measurement of activity of LS-samples. It consists of a three PMT LS counting detector and a 5 mm x 5 mm x 1 mm Cadmium Telluride (CdTe) γ-ray detector. The PMTs in the LS counting system are square, small form-factor Hamamatsu R7600-200

*Corresponding author
Email address: ch.dutsov@phys.uni-sofia.bg (Chavdar Dutsov)

tubes with 350 ps FWHM transient time spread (Hamamatsu, 2016). The solid state detector is an AmpTek XR-100CdTe with a PX2T power supply and shaping amplifier (Amptek, 2020). The three PMTs are positioned with 120° displacement around a standard 20 ml liquid scintillation vial. The vial is placed in a 3D printed optical chamber made with polylactic acid (PLA) plastic. The chamber is covered with reflective polymer foil with 98.5% reflectivity across the visible spectrum (3M, 2021). The CdTe detector is placed as close as possible to the vial (≈ 2 mm), in order to achieve maximum geometrical efficiency and between 2 of the 3 PMTs (Figure 1). The detailed specification and performance of the device will be detailed in a future paper.

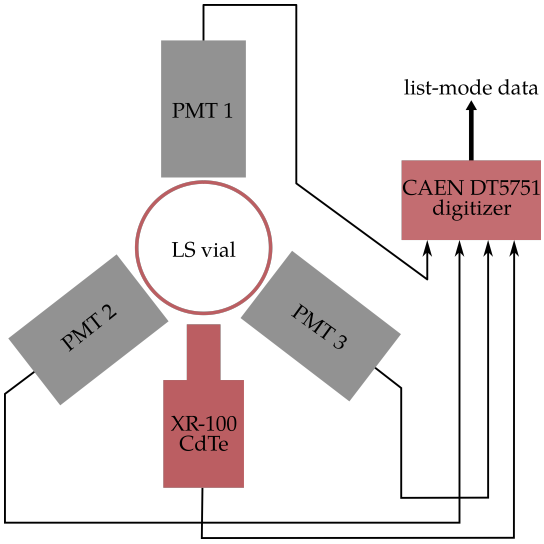

Figure 1: Simplified schematic of the 3-PMT LS counting detector and the CdTe γ-detector.

The three PMT channels and the amplified and shaped output of the CdTe detector are connected to a CAEN DT5751 desktop digitizer (CAEN, 2020) with 1 GS/s sampling rate. The signals of the three PMTs and the CdTe detector are digitized. A timestamp of the arrival times as well as the integrated charge are recorded for each event in a file for off-line analysis.

2.2. 2-PMT LS detection system

The second experimental system is an in-house developed LS counting detector with two XP2020Q PMTs looking from opposite sides at a standard 20 ml LS sample. The vial is placed in a 3D printed optical chamber which is optimized for fast light collection. This chamber was also covered with the same reflective polymer foil. Both PMTs are directly connected to the DT5751 digitizer and the incoming events are recorded in a list mode file. This system was used for the LS-LS coincidence counting measurements and to obtain the half-lives of the excited states without the use of the gamma channel.

2.3. Measured sources and data analysis software

The two detector systems were used to measure LS-sources of ^{57}Co (5 kBq) and ^{241}Am (1.2 kBq) in UltimaGold cocktails in standard 20 ml glass vials covered with diffusive tape. The latter is done in order to reduce the total internal reflection and trapping of light inside the sample. The diffusive tape was used consistently in all of the described measurements. Both sources contain approximately 100 µl water dissolved in 10 ml LS cocktail.

The data produced by the digitizer is analysed off-line using an in-house developed computer software that counts the coincidences between the channels and applies an extendible dead-time (20 µs base duration) after the end of the coincidence resolving time. The extendible dead-time ensures that enough time has passed after each detected signal such that no afterpulses are detected. The code was already tested and used for the study of coincidence counting algorithms (Dutsov et al., 2019) and the time response of different LS cocktails (Dutsov et al., 2020a). The list-mode data analysis software can output the time interval distributions between the PMT channels as well as between a PMT channel and the CdTe detector. The time interval between two channel, e.g., PMT A and PMT B or PMT C and CdTe, is considered as the time between the first detected events in the reference channel and in the secondary channel within a given coincidence window. The coincidence window used in the analysis of all measurements is 5000 ns. It is large enough to include more than 20 half-lives of the studied excited states. After such a long period, the amount of true coincidences will be negligible and all remaining observed coincidences can be considered accidental. The coincidence resolving time is also large enough to see the plateau formed by the accidental coincidences, that can be used to estimate their contribution and correct for it.

Due to the higher delay of the CdTe detector, the PMT channels in the 3-PMT detector are delayed by 4 µs using the software. This value was determined by measuring the ^{241}Am LS-source and changing the delay until a maximum coincidence counting rate is reached between one of the PMT channels and the γ channel with a 40 ns coincidence window. The timing of the PMTs was not adjusted relative to each other as they have almost identical timing properties and the static delay between them is less than a nanosecond.

2.4. Decay curve analysis

When analyzing the time interval distributions, depending on the measurement conditions, it is possible that the observed decay constant differs from the true decay constant of the excited state. Such a problem could arise when there is a large probability for uncorrelated events to serve as stop signals. This was first described by Radeloff et al. and they have proposed that a bi-exponential equation is needed in such cases to accurately describe the observed decay curve. The equation is the following (Radeloff et al., 1967):

$$N_{\text{total}}(t)dt = Ae^{-(N_2+\lambda)t}dt + Be^{-N_2 t}dt, \qquad (1)$$

where $N_{\text{total}}(t)dt$ is the number of detected events per unit time, λ is the decay constant of the excited state and N_2 is the counting rate in the channel of the transition depopulating the excited state. The second term in the sum accounts for contribution of the accidental coincidences and background signals to the observed time interval distribution. The first term is an exponential decay with a modified decay constant in order to account for uncorrelated events that stop the time measurement prematurely. This behaviour was found to be significant for measurements of half-lives in the order of a second.

The highest single counting rate and the longest half-life studied in this paper are for the 14.4 keV level of ^{57}Fe, so if the effect is significant it will be most pronounced in this measurement. The counting rate in the stop channel is $N_2 = 1.3 \times 10^3$ s^{-1} and the decay constant of the excited state is $\lambda = 7.094 \times 10^6$ s^{-1}. The difference between the apparent decay constant and the true one is 0.02%. As this is negligible compared to the other uncertainty factors a single exponent with λ as an argument was used to fit all obtained time distributions.

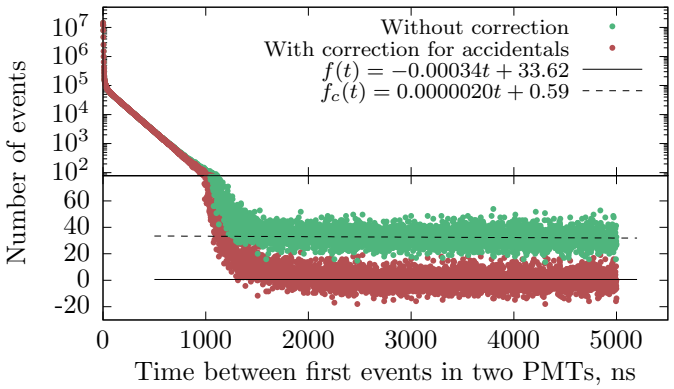

Figure 2: Time interval distribution of a ^{57}Co source without and with correction for accidental coincidences. The points between 3 µs and 5 µs were considered for the linear fits. Please note that bins with less than 80 detected events are shown in linear scale and with more than 80 in logarithmic scale. The measurement time is 60 hours.

However, the accurate determination of the half-life necessitates that the plateau that is formed by the accidental coincidences is taken into account. In equation (1) this is done via the second term in the sum. In this study all time interval distributions are corrected for accidental coincidences according to the experimental method described in (Dutsov et al., 2020b). The distribution is obtained for a large enough window that includes all correlated coincidences as well as a part of the distribution which contains only accidental coincidences. The distribution of the accidental coincidences is approximated with a linear function $f(t) = a_0 x + a_1$ and the accidental coincidences are subtracted from the observed time interval distribution to produce the distribution of the true coincidences. The approximation with a linear function is valid in the studied cases as the counting rate is low enough. The procedure is illustrated in Figure 2. The time interval distribution of a ^{57}Fe LS-source with start and stop signals from an LS detector is shown before and after subtraction of the contribution of the accidental coincidences. The distribution after the subtraction of the accidental coincidences was again fitted with a linear function $f_c(t) = b_0 x + b_1$, to illustrate that after the correction their contribution is negligible.

The obtained time interval distributions are fitted with the non-linear least squares Levenberg-Marquardt algorithm using `gnuplot` (gnuplot, 2020). The number of events per bin is in all cases more than 30 and so we can assume that the statistical fluctuations have a Gaussian distribution. The standard deviation of the number of detected events in each bin is calculated as the square root of the number of events in the bin. The uncertainty of each data point is taken into account in the fitting algorithm. The size of each bin is 1 ns. The uncertainty on the fit parameters (e.g., the decay constant) reported by the fitting algorithm are the parameter error estimates which are readily obtained from the variance-covariance matrix after the final iteration of the Levenberg-Marquardt algorithm.

3. Results

3.1. Half-life measurements of excited states in ^{57}Fe

^{57}Co decays via EC to the 136.5 keV excited level of ^{57}Fe with 99.8% probability (shown in Figure 3). This decay is attended by the emission of X-rays, Auger electrons, and/or conversion electrons, which are detected in the liquid scintillator. The time for the rearrangement of electrons after the EC is in the order of 10^{-16} s and thus this process is considered to be instant compared to the studied half-lives (Briand et al., 1996). The energy released in the scintillator after the EC is in the range from 5.4 to 7.1 keV. The detection efficiency for a double coincidence in the LS counting detector for such energies is around 50%.

The second excited level of ^{57}Fe transitions to the ground level with 10.7% emission intensity of γ-rays or to the first excited level with 85.5% emission intensity of γ-rays with a half-life of around 8.6 ns (see Figure 3). The 2–0 transition can be detected in the scintillator by the 129.4–136.5 keV conversion electrons, produced with about 4% probability, or it can be detected via the gamma emission due to the transition $\gamma_{2,0}$(Fe) = 136.5 keV which directly interacts with the scintillator by Compton scattering or photoelectric effect. Similarly to the previous transition, the 2–1 transition can be detected via the 115–122 keV conversion electrons, produced with about 4% probability, or via the gamma emission due to the transition $\gamma_{2,1}$(Fe) = 122 keV. Finally, the first excited level has a 98 ns half-life and the 1–0 transition can be detected via the 7.3–14.4 keV conversion electrons or gamma emission due to the transition $\gamma_{1,0}$(Fe) = 14.4 keV (Bé et al., 2016).

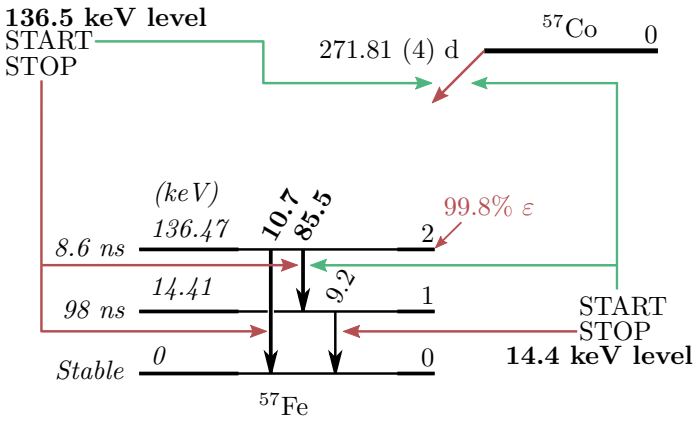

Figure 3: A simplified decay scheme of ^{57}Co. Only gamma emissions with intensities above 0.2% are shown. The START and STOP signals that were used to study the half-lives of the two excited states are also shown. Data and figure adapted from (Bé et al., 2016).

With the analysis of this decay scheme and the properties of this specific LS-γ detector, there are a few possible start-stop combinations from the available events:

1. EC is detected (START) and $\gamma_{2,0}$(Fe) is detected (STOP). Such coincidences were used to study the half-life of the 2$^{\text{nd}}$ excited state.
2. EC is detected (START) and $\gamma_{2,1}$(Fe) is detected (STOP). In this case $\gamma_{1,0}$(Fe) would be within the dead time of the detector. These coincidences were also used to study the half-life of the 2$^{\text{nd}}$ excited state.
3. EC is not detected; $\gamma_{2,1}$(Fe) is detected (START) and $\gamma_{1,0}$(Fe) is detected (STOP). This was used to study the half-life of the 1$^{\text{st}}$ excited state.
4. EC is detected (START), $\gamma_{2,1}$(Fe) is not detected (low probability) and $\gamma_{1,0}$(Fe) is detected (STOP). Such coincidences were also used to study the half-life of the 1$^{\text{st}}$ excited state.

The various start and stop possibilities are shown in Figure 3.

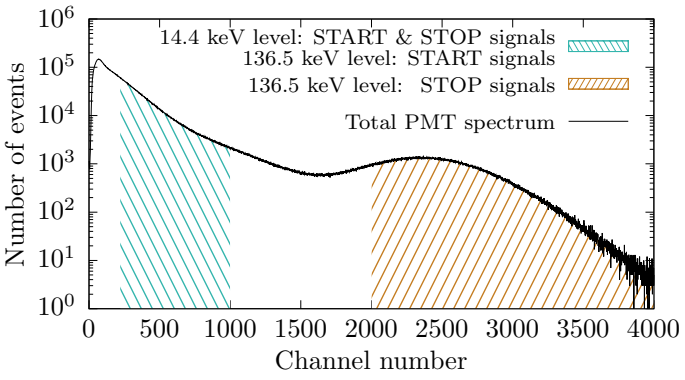

Figure 4: Spectrum of the ^{57}Co LS-sample obtained with the 2-PMT system. For the study of the 14.4 keV level the START and STOP signals are taken from the lower energy part of the spectrum. For the study of the 136.5 keV level the low energy events are used as START and the high energy events are used as STOP.

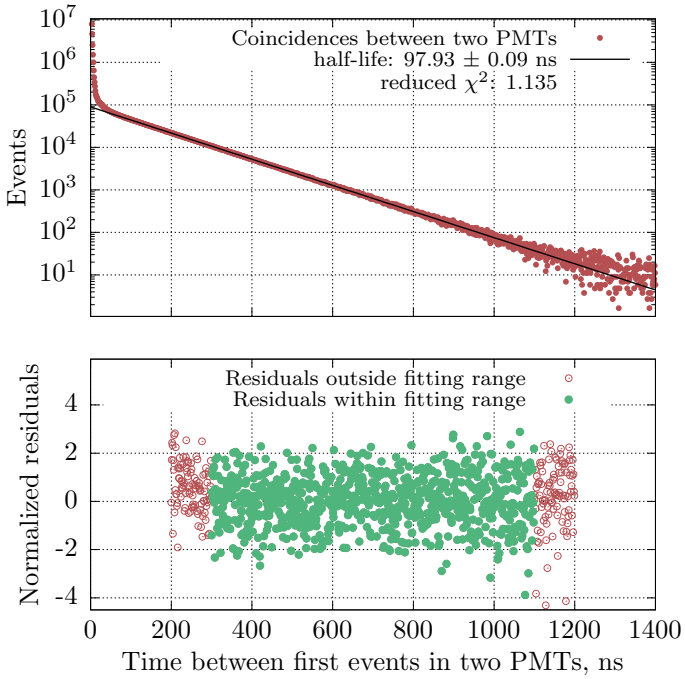

Figure 5: LS-LS coincidence counting measurements of the 14.4 keV level of ^{57}Fe. The start signal is given by a low energy event in one PMT and a low energy event in the other PMT. The time interval distribution is obtained with the 3-PMT detector. The normalized residuals are in units of number of standard deviations.

Half-life measurement of the 14.4 keV level of ^{57}Fe using LS-LS coincidence counting. A 60 hour long measurement of the 5 kBq ^{57}Co LS-source was performed using the 3-PMT & γ detection system. This system was preferred over the 2-PMT system in order to directly compare results with LS-γ coincidence counting on the same list-mode data. The obtained list-mode files were analysed using the dedicated software; two of the PMT channels were constrained to include only events with medium energy - i.e. removing single photon events and the high-energy 122-136 keV interactions. Removal of the single photon events is done in order to remove spurious events and delayed fluorescence coming from the cocktail. The energy spectrum and the part of the events which were considered for this study are shown in Figure 4. Even after selecting only a part of the energy spectrum that excludes the high energy events all coming from the 2$^{\text{nd}}$ excited state of ^{57}Fe there is a non-zero probability to detect events from this state because of Compton scattered electrons from the $\gamma_{2,0}$(Fe) and $\gamma_{2,1}$(Fe) transitions. Such events will distort the decay curve of the 1$^{\text{st}}$ excited state as they can serve as both start and stop signals. However, after ten half-lives of the 8.6 ns level, or about 90 ns, only events from the 14.4 keV level can be detected as a stop signal due to its significantly longer life-time compared to the other transitions.

Another effect that has to be considered is that the Compton scattered electrons produced from the $\gamma_{2,1}$(Fe) transition interacting with the cocktail can act as a start signal. Due to the 8.6 ns half-life of the 2$^{\text{nd}}$ excited state

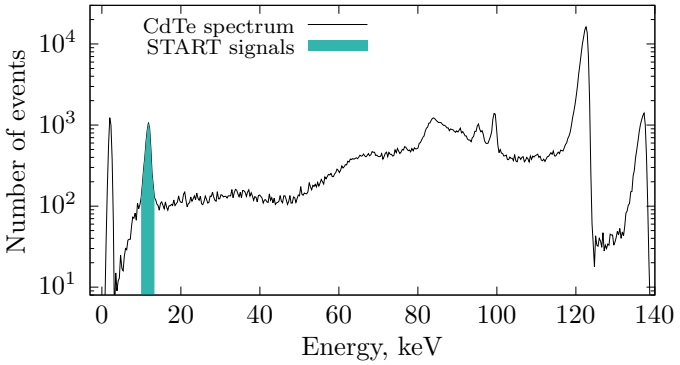

Figure 6: Spectrum of the ^{57}Co LS-sample obtained with the CdTe γ-ray detector. The events in the 14.4 keV peak were used as a start signal in the LS-γ measurements.

they cannot be considered to be instantaneous after the decay. This leads to a sum of two exponential distributions: first a rise time equal to the decay time of the 2$^{\text{nd}}$ excited state and second an exponential decay with the decay constant of the 1$^{\text{st}}$ excited state. After a sufficient time the effect of the rise time is negligible and only the decay time of the 2$^{\text{nd}}$ excited state will be observed.

The time interval distribution between the first events in two PMTs within the selected energy range is shown in Figure 5. The total number of coincidence events in the presented measurement is 10^8. The time distribution was fitted with an exponential decay and the points considered in the fit are between 300 and 1100 ns. The obtained half-life is 97.93(9) ns, where the uncertainty is only the uncertainty reported by the fitting algorithm. The residuals are well grouped within $\pm 2\sigma$. Some residuals outside of the fit boundaries are also shown in order to illustrate that the quality of the fit is preserved also at wider range.

Measurement of the 14.4 keV level of ^{57}Fe using LS-γ coincidence counting. The same list-mode data of the ^{57}Co measurement was used in order to study the LS-γ coincidence counting. In this case the start signal is given by an event in the 14.4 keV peak in the CdTe detector and the stop by a low-energy event (excluding the single photon peak) in one of the three PMTs, PMT B, chosen for its slightly larger quantum efficiency. The energy spectrum in the CdTe is shown in Figure 6. The time interval distribution is displayed in Figure 7. The fit is performed between 250 and 450 ns with an exponential function. The obtained half-life is 97.8(28) ns, where the uncertainty is only the uncertainty reported by the fitting algorithm. Due to the low geometrical efficiency of the γ-channel detector, it is difficult to obtain the same precision for the same measurement time as with the LS-LS coincidence counting method.

Measurement of the 136.5 keV level of ^{57}Fe using LS-LS coincidence counting. The half-life of the 136.5 keV excited state was determined from LS-LS coincidence counting using the 2-PMT detector by triggering on medium-energy events in one PMT as a start signal and using high-energy events as a stop signal in another PMT. The ^{57}Co LS-source was measured for 62 hours.

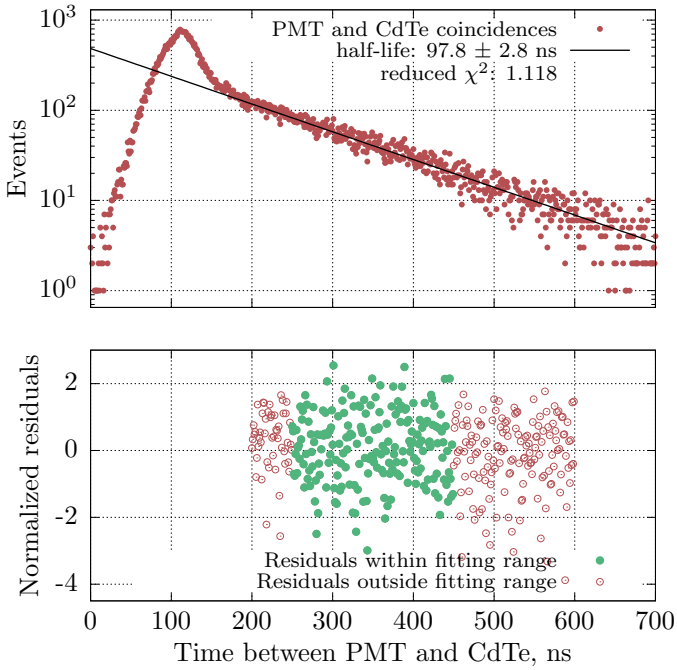

Figure 7: ^{57}Co LS-γ coincidence counting. Start signal is given by the 136 keV peak in the CdTe and the stop is given by a low-energy PMT event. The normalized residuals are in units of number of standard deviations.

The spectrum of the events considered for start and stop is shown in Figure 4. The study of the 2$^{\text{nd}}$ excited state is significantly easier compared to the 1$^{\text{st}}$ as there is only one start event and the two stop transitions 2–1 and 2–0 can be separated well from the rest. The half-life of this level is too short to be studied with the gamma detector due to its timing resolution.

The observed decay curve in such a configuration is shown in Figure 8. The fast response of the PMTs in LS-LS technique allows us to study 9.7 half-lives of this state. The half-life obtained from an exponential fit is 8.78(2) ns, where the uncertainty is only the uncertainty reported by the fitting algorithm.

3.2. Measurement of the half-life of the 59.54 keV level of ^{237}Np

^{241}Am decays with the emission of an α-particle to the 59.54 keV short lived isomeric state of ^{237}Np with 84.45% probability (see Figure 9). The 1 kBq source of ^{241}Am in UltimaGold (UG) liquid scintillator in a standard 20 ml glass vial was prepared for the purpose of this study. Two measurements of this source were performed on the two detector systems. The source was measured for 136 hours with the 3-PMT & γ measurement system and the events from all PMT channels and the γ detector were recorded in list-mode files. The files were analyzed to obtain the time

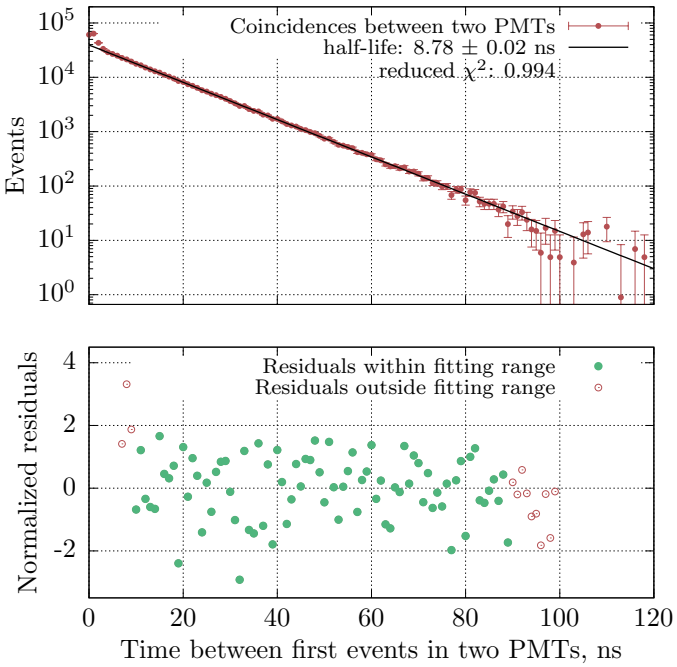

Figure 8: LS-LS coincidence counting measurements of the 136.5 keV level of ^{57}Fe. The start signal is given by a low energy event in one PMT and a 122-136 keV event in the other PMT. The time interval distribution is obtained with the 2-PMT system. The normalized residuals are in units of number of standard deviations.

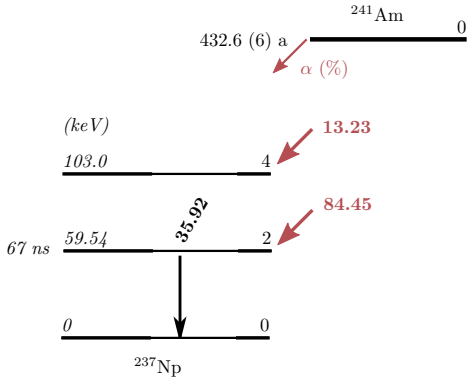

Figure 9: Simplified decay scheme of ^{241}Am. Only transitions with intensities above 3% are shown. Data and figure adapted from (Bé et al., 2016).

interval distributions from the LS-γ coincidence counting. The source was also measured with the 2-PMT system in order to obtain the time interval distribution from the LS-LS coincidence counting. Unfortunately, due to time constraints, only a 1 hour long measurement on this system was available.

For the usual applications of the LS counting systems the PMTs are working in single photon mode with gain in the order of 10^7. At such high gain the light from the alpha particles of ^{241}Am would produce large signals with significant afterpulses spanning several microseconds. Thus, single photon mode would be unsuitable to detect

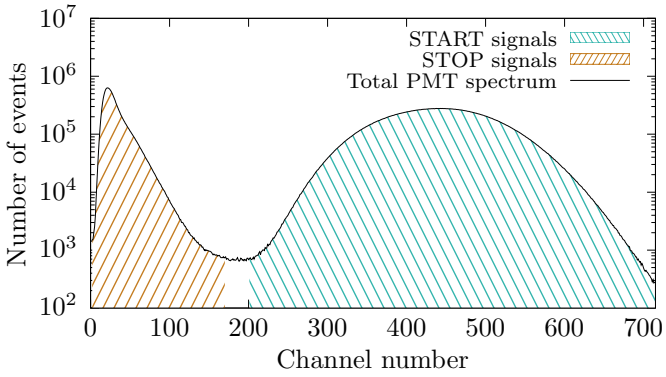

Figure 10: Spectrum of the ^{241}Am LS-sample obtained with the 2-PMT system. The ^{241}Am α peak is shown in green and the events from the 59.5 keV transition of ^{237}Np in cyan.

the signal from the 59.54 keV de-excitation as the detectors will be saturated. This saturation can be avoided by reducing the PMT high-voltage, from 2100 V to 1700 V for the used XP2020Q PMTs, thereby reducing the gain to approximately 10^5. This is sufficient to reduce the afterpulses to a negligible level and gives the opportunity to use the ^{241}Am α-particle in the scintillator as a start signal and a 59.54 keV conversion electron or γ, again in the scintillator, as a stop.

The raw data from the digitizer contains the timestamps and energy of all recorded events, excluding events separated by a time shorter than the trigger hold-off, which was set to 32 ns. In the analysis of all measurements the coincidence window is 5000 ns and the dead-time is 20 microseconds. In the LS-LS measurements of the 59 keV level, the start signals are high-amplitude alpha events in one PMT and the stop signals are low-energy gamma events in the other PMT (see Figure 10). Thus, even though both PMTs detect the alpha event, it is discarded in one of the PMTs due to the energy gate and only the 59.5 keV event is processed. This happens within the coincidence window and before the imposed dead-time.

The obtained decay curve with such a configuration is shown in Figure 12. A major advantage of the LS-LS coincidence counting with the 2-PMT detector over using a γ detector is the 100% efficiency for α-particles and close to 100% efficiency for the 59.54 keV emissions.

The result from the LS-LS coincidence counting method was compared with the half-life obtained with LS-γ coincidence counting method using the 3-PMT & γ detector. In this case the start signal is given by an α event in the scintillator and the stop event is given by an event in the 59.54 keV peak in the CdTe detector.

The alpha particle coming from the decay ^{241}Am is detected in the scintillator with 100% efficiency. The 59.54 keV gamma can then be detected in the CdTe detector with a geometrical efficiency of about 0.3%. The CdTe spectrum is shown in Figure 11. The performed measurement is 136 h long and the total number of recorded coincidences is 4×10^5. The distribution of the time interval

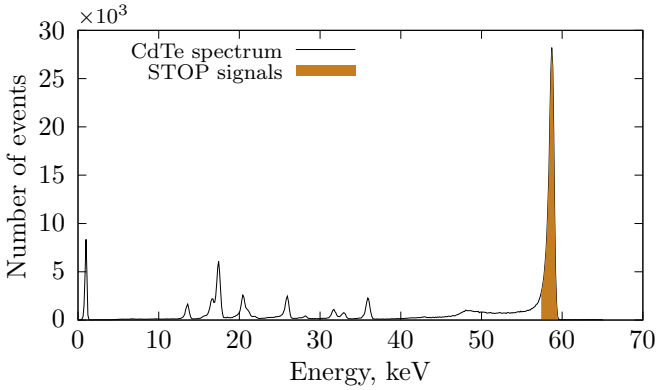

Figure 11: Spectrum of the ^{241}Am LS-sample obtained with the CdTe γ-ray detector. The events in the 59.54 keV peak were used as a stop signal in the LS-γ measurements. The left tailing of the peak is due to incomplete charge collection in the CdTe.

between a PMT event and the CdTe detector event in the 59.54 keV peak is displayed in Figure 13. The number of events per bin are normalized by the total number of detected events. The bottom graph shows the residuals of the fit within the fitting range of 150 ns to 500 ns in red and outside the fitting range in green. The points before 150 ns are excluded in order to remove effects of the gaussian timing response of the CdTe and events after 500 ns are excluded due to too low statistics. The reduced χ^2 statistic of the fit is 1.037. The observed half-life is 67.60(22) ns, where the uncertainty is only the uncertainty reported by the fitting algorithm.

3.3. Analysis of the results and uncertainty evaluation

An overview of the uncertainty budgets is presented in Table 1. The factors that could influence the half-life assessment considered in this work are: the uncertainty associated with the fitting algorithm, the corrections for accidental coincidences, the choice of boundaries for the fitting and possible contribution from other excited states in the case of LS-LS coincidence counting method. The fits of the decay curves were performed with non-linear least squares Levenberg-Marquardt algorithm. The fit uncertainties are taken from the output of the fitting algorithm. The uncertainty associated with the correction for accidental coincidences was estimated by a manual change of their amplitude until a visible change in the residuals was observed; similar to the technique described in (Suliman et al., 2013). The uncertainty coming from the choice of fitting boundaries was evaluated by choosing different low and high limits and studying the effect on the final value for the half-life. For the LS-LS coincidence counting method there is some uncertainty due to the choice of the parts of the PMT spectrum that are taken for start and stop signals. The estimate of this uncertainty was performed by analyzing the decay curves obtained with different parts of the spectra for the start and stop energy windows.

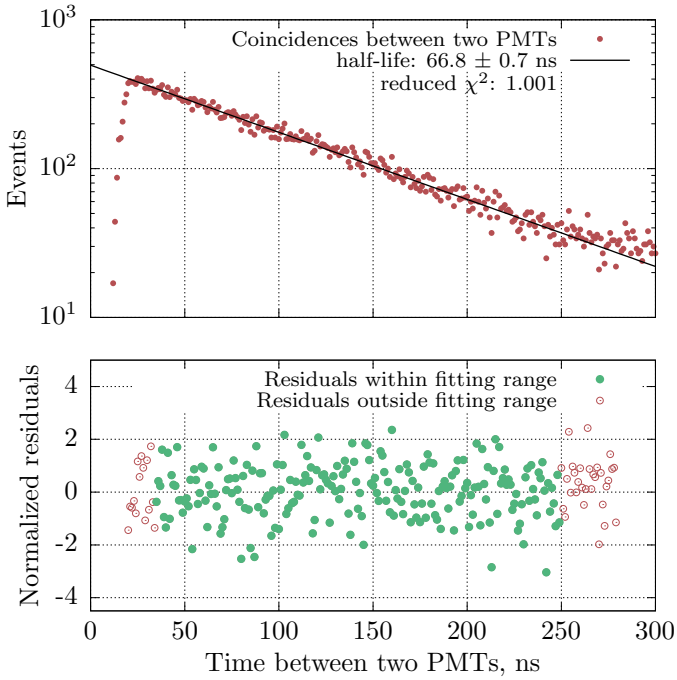

Figure 12: LS-LS coincidence counting measurement of the 59.5 keV level of ^{237}Np. The start signal is given by events in the alpha peak of the LS spectrum and the stop signal is given by a low energy event from the 59.5 keV transition. The time interval distribution is obtained with the 2-PMT system. The normalized residuals are in units of number of standard deviations.

Due to the poor energy resolution of the LS counter it is important to consider that the studied excited states could be populated by higher-lying states. Their half-life is in some cases unknown and should not be readily assumed to be instant compared to the half-life of the studied state. In the case of the 136.5 keV level of ^{57}Fe there are two higher energy excited states from which it could be populated. The 3–2 and the 4–2 transition have 0.0004% and 0.015% probability respectively and would give negligible contribution to the decay curve observed in Figure 8. For the 14.4 keV level of ^{57}Fe the 3–1 transition has 0.0032% probability and according to the evaluation given in the Evaluated Nuclear Structure Data File (ENSDF) (Bhat, 1992) the half-life of the 3$^{\text{rd}}$ excited state is less than 4 ns. Therefore, this transition will have a negligible influence on the decay curve observed in Figure 5. The 4–1 transition, however, occurs with 0.159% probability and its energy is 692.4 keV. The half-life of the 4$^{\text{th}}$ excited state is, however, unknown. The maximum deviation in the obtained decay time due to this transition would be less than 0.05% if we conservatively assume that the 4$^{\text{th}}$ excited state has close to 50 ns half life. No such considerations are needed in the case of the ^{237}Np decay curve from LS-γ coincidence counting method as the start and stop levels are well defined.

The final values obtained for the half-lives of the two ^{57}Fe states and the ^{237}Np state, after taking into account the factors contributing to the uncertainty, are shown in

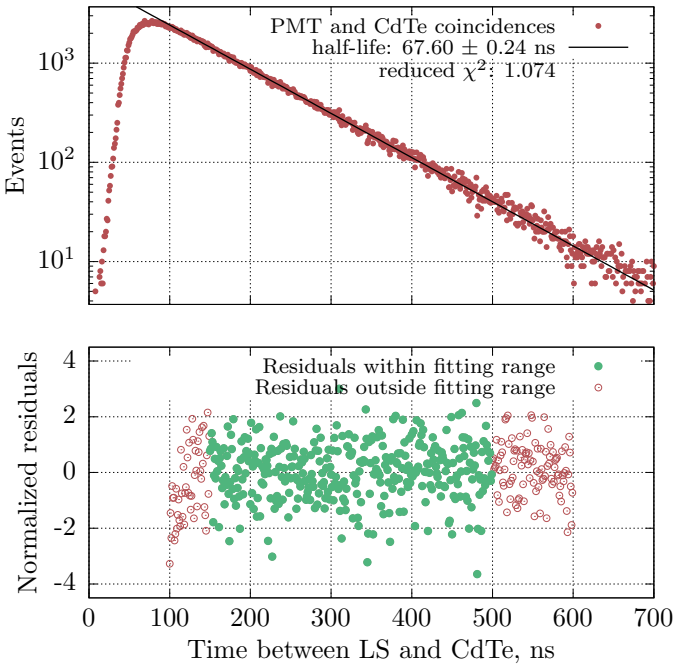

Figure 13: LS-γ coincidence counting measurement of the 59.5 keV level of ^{237}Np. The start signal is given by the alpha particle in the scintillator and the stop is given by an event in the 59.5 keV peak in the CdTe. The normalized residuals are in units of number of standard deviations.

Table 1. Due to the low counting statistics the ^{237}Np LS-LS and the ^{57}Fe LS-γ measurements were not considered for the final result report (last row of Table 1).

Comparison with existing decay data. The Decay Data Evaluation Project (DDEP) data on ^{57}Co provides 98.0(4) ns for the half-life of the 14.4 keV level of ^{57}Fe (Kellett and Bersillon, 2017; Bé et al., 2016). It is taken as the weighted average of 7 measurements presented in Table 2.

It should be noted that there is a significant discrepancy between the different measurements. The obtained half-life value in this work is 97.9(4) ns which is in agreement with reports 1 and 3 within the estimated uncertainties, but not with reports 4 and 6; reports 2, 5 and 7 have large uncertainties, and thus are in agreement. Thus, the new results obtained in this study would bring an improvement to the dataset and may be considered in future evaluations of the half-life of the 14.4 keV level of ^{57}Fe.

The DDEP data on ^{57}Co states 8.6(4) ns for the half-life of the 136.5 keV level of ^{57}Fe. It is taken as the weighted average of 5 measurements, that are consistent within their stated uncertainties. The result from this study, 8.78(4) ns, has the lowest uncertainty compared to previous measurements and is consistent with the already provided average value.

The Nuclear Decay Sheets (NDS) state 68.1(2) ns for the half-life of the 59.54 keV level of ^{237}Np (Basunia, 2006). The value is the weighted average of 5 measurements, the most recent of which is from 1972. The value obtained in this study does not agree with the stated average value, which could be caused by the very low uncertainty of the 1972 measurement 68.3(2) ns (Miller et al., 1972). In the ENSDF evaluation (Bhat, 1992), the same 5 measurements were used, but the low uncertainty of the 1972 measurement by Miller et al. is increased to 0.7 ns (1%) by the evaluator. The obtained weighted average value is 67.2(7) ns, which is consistent with the result obtained in this work. The DDEP half-life value for the same level is 67(2) ns and is based on just one measurement. Due to its large uncertainty, it is consistent with the value obtained in the current study. As the latest measurements of this half-life that can be found in the current evaluations are 49 years old, the value obtained in this work will present an improvement in the dataset.

4. Conclusions

The half-lives of two excited nuclear states in ^{57}Fe and one in ^{237}Np were measured in the presented study by means of LS-LS and LS-γ coincidence counting methods. The half-life of the 59.54 keV level of ^{237}Np was measured by LS-γ coincidence counting and the result is 67.60(25) ns, which is in good agreement with the ENSDF decay data. The half-life of the 14.4 keV level of ^{57}Fe was measured by LS-LS coincidence counting and the result is 97.9(3) ns which is consistent with some of the published results, however a significant discrepancy exist between the values found in the literature. The half-life of the 136.47 keV level of ^{57}Fe was measured also by the LS-LS coincidence counting method and the result is 8.78(4) ns, which is consistent with the published data and comes with a significant improvement in the uncertainty. The results presented in this paper could be very valuable for future evaluations of the half-lives of the studied excited states.

Liquid scintillation fast timing measurements can be a useful tool to refine some already known decay times. An advantage over more-commonly used methods is the relatively short measurement time that is needed, due to the 4π geometrical efficiency. This could allow more precise studies of half-lives of excited states of short lived nuclides where long measurements are difficult to perform, and to isotopes in liquid phase. The method employing LS-LS coincidence counting is shown be useful for precise measurements of half-lives as short as 8 ns. One drawback over the LS-γ coincidence counting method is the limited energy resolution as the detection of γ-rays provides a better selectivity than LS counting.

Acknowledgements

The authors like to express their gratitude towards Xavier Mougeot, PhD, for his valuable input on the subject and to Sophie Morelli for the preparation of the ^{57}Co source.

Table 1: Measured half-life values and uncertainty budgets. The uncertainty values are the standard uncertainties. Note that the LS-LS measurement of the ^{237}Np source is only 1 h long, compared to the 136 h LS-γ measurement. Due to the low counting statistics and high fit uncertainties the LS-γ measurement of the 14.4 keV level of ^{57}Fe and the LS-LS measurement of the 59.5 keV level of ^{237}Np were omitted in the final result.

	136.5 keV ^{57}Fe	**14.4 keV ^{57}Fe**		**59.5 keV ^{237}Np**	
	LS-LS	LS-γ	LS-LS	LS-γ	LS-LS
Uncertainty from fit	0.22%	2.9%	0.13%	0.33%	1.1%
Corrections for accidental coincidences	0.25%	0.05%	0.15%	0.15%	0.50%
Fitting boundaries	0.22%	0.10%	0.24%	0.10%	0.20%
Contribution from higher excited states	$\leq$ 0.01%	$\leq$ 0.01%	0.05%	–	–
Choice of gates in the spectrum	0.10%	0.10%	0.25%	$\leq$ 0.01%	$\leq$ 0.01%
Total	0.41%	2.9%	0.40%	0.37%	1.2%
Measured half-life	8.780(36) ns	97.8(28)	97.90(40) ns	67.60(25) ns	66.80(78) ns
Final result	**8.780(36) ns**	**97.90(40) ns**		**67.60(25) ns**	

#	Citation	Value, ns
1	(Clark, 1961)	97.9(2)
2	(Kistner and Sunyar, 1965)	98.0(10)
3	(Eckhause et al., 1966)	97.7(2)
4	(Hohenemser et al., 1969)	99.3(5)
5	(Alikov et al., 1978)	97.8(14)
6	(Ahmad et al., 1995)	99.2(4)
7	(Morozov et al., 2006)	94.0(40)

Table 2: Previous measurements of the half-life of the 14.4 keV level of ^{57}Fe. The table is adapted from the DDEP evaluation for that nuclide (Kellett and Bersillon, 2017; Bé et al., 2016).

The experiments for this work were performed during the stay of Ch. D. at LNHB with a financial support from the French Laboratoire national de métrologie et d'essais (LNE). This financial support is gratefully acknowledged.

This work is supported by the Bulgarian National Scientific Research Fund under contract № KP–06–H38/9 from 06.12.19 (TDCX).

References

3M. 3M enhanced specular reflector (3M ESR). https://www.3m.com/3M/en_US/p/d/eebgdar000006/, 2021. Accessed on 16.05.2021.

I. Ahmad, K. E. Rehm, E. P. Kanter, W. Kutschera, W. R. Phillips, and A. R. Barnett. Half-lives of isomeric states in ^{57}Fe and ^{83}Kr. *Physical Review C*, 52(4):2240–2241, Oct. 1995. doi: 10.1103/physrevc.52.2240. URL https://doi.org/10.1103/physrevc.52.2240.

B. A. Alikov, Y. Babryshchuk, G. I. Lizurei, K. M. Muminov, T. M. Muminov, Y. Salikhbaev, and R. R. Usmanov. *Journal of the Joint Institute for Nuclear Research*, 13(P13):10911, 1978.

Amptek. AMPTEK, X-Ray and gamma ray detector high resolution CdTe Cadmium Telluride, XR-100T-CdTe. http://www.amptek.com, 2020. Accessed on 16.05.2021.

M. S. Basunia. Nuclear data sheets for A = 237. *Nuclear Data Sheets*, 107(8):2323–2422, Aug. 2006. doi: 10.1016/j.nds.2006.07.001. URL https://doi.org/10.1016/j.nds.2006.07.001.

M. M. Bé, V. Chisté, C. Dulieu, M. A. Kellett, X. Mougeot, A. Arinc, V. P. Chechev, N. K. Kuzmenko, T. Kibédi, A. Luca, and A. L. Nichols. *Table of Radionuclides*, volume 8 of *Monographie BIPM-5*. Bureau International des Poids et Mesures, Pavillon de Breteuil, F-92310 Sèvres, France, 2016. ISBN 978-928-222-2-6-4-5. URL http://www.bipm.org/utils/common/pdf/monographieRI/Monographie_BIPM-5_Tables_Vol8.pdf.

M. R. Bhat. Evaluated nuclear structure data file (ENSDF). In *Nuclear Data for Science and Technology*, pages 817–821. Springer Berlin Heidelberg, 1992. doi: 10.1007/978-3-642-58113-7_227. URL https://doi.org/10.1007/978-3-642-58113-7_227.

J.-P. Briand, B. d'Etat Ban, D. Schneider, M. A. Briere, V. Decaux, J. W. McDonald, and S. Bardin. Time for the emptyLshell of a hollow atom to be filled. *Physical Review A*, 53(4):2194–2199, Apr. 1996. doi: 10.1103/physreva.53.2194. URL https://doi.org/10.1103/physreva.53.2194.

CAEN. CAEN DT5751 digitizer manual. https://www.caen.it/products/dt5751/, 2020. Accessed on 16.05.2021.

J. Chmeleff, F. von Blanckenburg, K. Kossert, and D. Jakob. Determination of the ^{10}Be half-life by multicollector ICP-MS and liquid scintillation counting. *Nuclear Instruments and Methods in Physics Research Section B: Beam Interactions with Materials and Atoms*, 268(2):192–199, Jan. 2010. doi: 10.1016/j.nimb.2009.09.012. URL https://doi.org/10.1016/j.nimb.2009.09.012.

M. A. Clark. Atomic Energy of Canada Limited Report AECL-1337. page 40, 1961.

C. Dutsov, K. Mitev, P. Cassette, and V. Jordanov. Study of two different coincidence counting algorithms in TDCR measurements. *Applied Radiation and Isotopes*, 154:108895, Dec. 2019. doi: 10.1016/j.apradiso.2019.108895.

C. Dutsov, P. Cassette, K. Mitev, and B. Sabot. In quest of the optimal coincidence resolving time in TDCR LSC. *Nuclear Instruments and Methods in Physics Research Section A: Accelerators, Spectrometers, Detectors and Associated Equipment*, page 164846, Nov. 2020a. doi: 10.1016/j.nima.2020.164846. URL https://doi.org/10.1016/j.nima.2020.164846.

C. Dutsov, P. Cassette, B. Sabot, and K. Mitev. Evaluation of the accidental coincidence counting rates in TDCR counting. *Nuclear Instruments and Methods in Physics Research Section A: Accelerators, Spectrometers, Detectors and Associated Equipment*, 977:164292, Oct. 2020b. doi: 10.1016/j.nima.2020.164292. URL https://doi.org/10.1016/j.nima.2020.164292.

M. Eckhause, R. J. J. Harris, W. B. Shuler, and R. E. Welsh. A measurement of the lifetime of the 14.4 keV level of ^{57}Fe. *Proceedings of the Physical Society*, 89(1):187–188, Sept. 1966. doi: 10.1088/0370-1328/89/1/130. URL https://doi.org/10.1088/0370-1328/89/1/130.

gnuplot. gnuplot fitting algorithms manual. http://gnuplot.

sourceforge.net/docs_4.2/node82.html, 2020. Accessed on 16.05.2021.

Hamamatsu. *Photomultiplier tubes R7600U series*. Hamamatsu photonics, 2016. URL https://www.hamamatsu.com/eu/en/product/type/R7600U-20/index.html. Accessed on 16.05.2021.

C. Hohenemser, R. Reno, H. C. Benski, and J. Lehr. Time-Differential Perturbed Angular-Correlation Experiment for ^{57}Fe in a Ni host and a comparison with the Mössbauer effect. *Physical Review*, 184(2):298–302, Aug. 1969. doi: 10.1103/physrev.184.298. URL https://doi.org/10.1103/physrev.184.298.

M. A. Kellett and O. Bersillon. The decay data evaluation project (DDEP) and the JEFF-3.3 radioactive decay data library: Combining international collaborative efforts on evaluated decay data. *EPJ Web Conferences*, 146:02009, 2017. doi: 10.1051/epjconf/201714602009.

O. C. Kistner and A. W. Sunyar. Excited states of ^{57}Fe populated in ^{57}Co decay. *Physical Review*, 139(2B):B295–B299, July 1965. doi: 10.1103/physrev.139.b295. URL https://doi.org/10.1103/physrev.139.b295.

K. Kossert. Half-life measurement of ^{212}Pb by means of a liquid scintillator-based ^{220}Rn trap. *Applied Radiation and Isotopes*, 125:15–17, July 2017. doi: 10.1016/j.apradiso.2017.03.026. URL https://doi.org/10.1016/j.apradiso.2017.03.026.

K. Kossert, G. Jörg, O. Nähle, and C. L. v. Gostomski. High-precision measurement of the half-life of ^{147}Sm. *Applied Radiation and Isotopes*, 67(9):1702–1706, Sept. 2009. doi: 10.1016/j.apradiso.2009.03.013. URL https://doi.org/10.1016/j.apradiso.2009.03.013.

K. Kossert, G. Jörg, and C. L. v. Gostomski. Experimental half-life determination of ^{176}Lu. *Applied Radiation and Isotopes*, 81:140–145, Nov. 2013. doi: 10.1016/j.apradiso.2013.03.033. URL https://doi.org/10.1016/j.apradiso.2013.03.033.

K. Kossert, M. P. Takács, and O. Nähle. Determination of the activity of ^{225}Ac and of the half-lives of ^{213}Po and ^{225}Ac. *Applied Radiation and Isotopes*, 156:109020, Feb. 2020. doi: 10.1016/j.apradiso.2019.109020. URL https://doi.org/10.1016/j.apradiso.2019.109020.

M. F. L'Annunziata. *Editor, Handbook of Radioactivity Analysis*. Academic Press, Elsevier., Amsterdam, The Netherlands, third edition, 2012.

G. H. Miller, P. Dillard, M. Eckhause, and R. E. Welsh. Determinations of nuclear level half-lives in ^{85}Rb and ^{237}Np and their use as timing standards. *Nuclear Instruments and Methods*, 104(1):11–12, Oct. 1972. doi: 10.1016/0029-554x(72)90290-x. URL https://doi.org/10.1016/0029-554x(72)90290-x.

V. A. Morozov, N. V. Morozova, T. Badica, G. Cata-Danil, D. Ghita, and I. V. Popescu. Measurement of the half-life for two ^{57}Fe excited states by a single-crystal scintillation time spectrometer. *Nuclear Instruments and Methods in Physics Research Section A: Accelerators, Spectrometers, Detectors and Associated Equipment*, 566(2):448–451, Oct. 2006. doi: 10.1016/j.nima.2006.06.059. URL https://doi.org/10.1016/j.nima.2006.06.059.

J. Radeloff, N. Buttler, W. Kesternich, and E. Bodenstedt. Measurement of lifetimes up to one second of isometric nuclear states populated in the decay of radioactive sources. *Nuclear Instruments and Methods*, 47(1):109–115, Jan. 1967. doi: 10.1016/0029-554x(67)90170-x. URL https://doi.org/10.1016/0029-554x(67)90170-x.

G. Suliman, S. Pommé, M. Marouli, R. V. Ammel, H. Stroh, V. Jobbágy, J. Paepen, A. Dirican, F. Bruchertseifer, C. Apostolidis, and A. Morgenstern. Half-lives of ^{221}Fr, ^{217}At, ^{213}Bi, ^{213}Po and ^{209}Pb from the ^{225}Ac decay series. *Applied Radiation and Isotopes*, 77:32–37, July 2013. doi: 10.1016/j.apradiso.2013.02.008. URL https://doi.org/10.1016/j.apradiso.2013.02.008.